Sphingosine Membrane Leaflets at Aqueous Interfaces

D. Vaknin
Ames Laboratory and Department of Physics and Astronomy,
Iowa State University, Ames, IA, U.S.A

Introduction

Lipids, the primary constituents of plasma and organelle membranes, form permeable walls and also impart appropriate settings for the action of membrane proteins. Some lipids, such as sphingolipids, were found to be active in the life-cycle of cells [1-3]. Sphingolipids are derived from C18-sphingosine (C18-SP), an amino alcohol with an acyl chain. Sphingosine is a secondary messenger that mediates the proliferation of mammalian cells [1, 2], whereas ceramide, an amide-linked fatty acid sphingosine (N-acyl-sphingosine), is a secondary messenger that mediates apoptosis (i.e., programmed cell death) [3]. It has been suggested recently that sphingolipids, together with other membrane constituents (i.e., cholesterol), form cohesive *lipid-rafts* that can mobilize membrane proteins [4]. Here, we briefly present synchrotron x-ray investigations of C18- and C20-SP (shown in Fig. 1) as they self-assemble at gas/water interfaces [5], thus extending our previous studies of C18-ceramide and C18-sphingomeylin [6, 7].

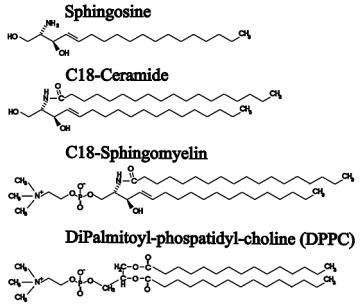

FIG. 1. Sphingosine and two of its derivatives, C18-ceramide and C18-sphingomyelin. Also, for comparison, a di-palmitoyl-phosphatidyl-choline (DPPC) is shown.

Methods and Materials

C18-SP ($C_{18}H_{37}O_2N$, molecular weight [MW] = 299.5) and C20-SP ($C_{20}H_{41}O_2N$, MW = 327.6, see Fig. 1) were obtained from Matreya, Inc. (Pleasant Gap, PA). Samples were weighed directly into volumetric flasks and subsequently filled with 2:1 chloroform/methanol (high-pressure liquid chromatography [HPLC]-grade, Fisher Scientific, Fair Lawn, NJ) and sonicated to form uniform solutions. Langmuir monolayers were prepared on pure water (Milli-Q apparatus, Millipore Corp., or Bedford, MA) in a temperature-controlled Teflon® trough maintained at 19 ±1°C and enclosed in a gas-tight aluminum container. Surface pressure was measured with a microbalance by using a filter-paper Wilhelmy plate. In order to reduce incoherent scattering from air and to slow film deterioration by oxidation due to production of radicals by the intense synchrotron beam, the monolayer was kept under a helium environment throughout the x-ray studies.

The liquid surface diffractometer at beamline station 6-ID-B at the APS was employed to investigate the structure of monolayers at air-water interfaces [8]. The highly monochromatic beam (16.2 keV; $\lambda = 0.765334$ Å), selected by a downstream Si double-crystal monochromator, is deflected onto the liquid surface to a desired angle of incidence with respect to the liquid surface by a second monochromator [Ge(220) crystal] located on the diffractometer. X-ray reflectivity (XR) and grazing incidence x-ray diffraction (GIXD) techniques are commonly used to determine the structure of monomolecular films on molecular length scales [8-10].

Results and Discussion

Corrugated Membrane Leaflets

Figure 2(A) shows normalized reflectivity curves, R/R_F (R_F is the calculated reflectivity from an ideally flat water interface) for both C18-SP and C20-SP monolayers. The solid lines are the best-fit calculated reflectivities based on the electron density (ED) profile models shown in Fig. 2(B). For C18-SP, two sets of measurements were performed, one for films spread with the intention to form a single layer by compression to a nominal molecular area of approximately 20 Å^2 (π of ~0), and the second in which the metastable procedure was used with excess material at the interface. Despite the fact that no significant surface pressure buildup was observed upon common compression (i.e., with no excess material at the interface), x-ray reflectivities of C18-SP films showed time-dependent deviations from the expected reflectivity of a pure water surface, providing evidence for the presence of varying amounts of C18-SP traces at the aqueous surface. This is consistent with pressure versus molecular area (π-A) isotherms, which show that natural C18-SP does not form a regular monolayer at the air-water interface because of finite solubility in water, but that it does leave residues at the gas-water

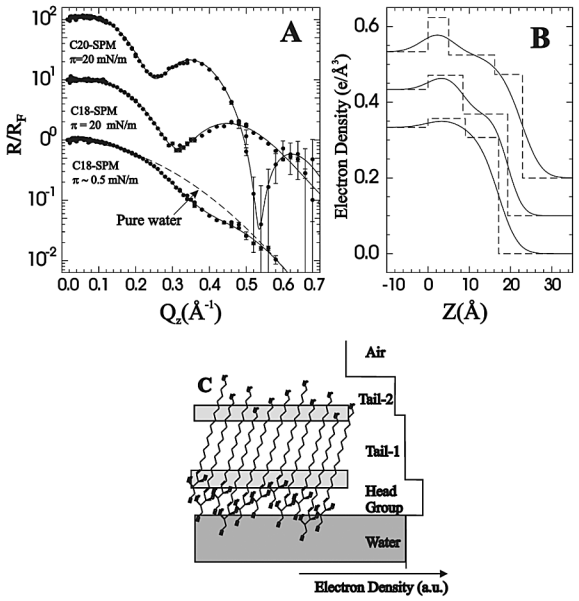

FIG. 2. A shows normalized reflectivities from monolayers of C20-SP (π = 20 mN/m) and of C18-SP (π at ≥0 mN/m and at 20 mN/m, spread in excess of a single layer). The dashed line is the reflectivity from water surface, showing the slight deviation of the reflectivity of C18-SP from that of pure water surface. B shows ED profiles (solid lines) used to calculate the reflectivities that best fit the data (solid lines in A). C is a schematic illustration of C20-SP monolayer and the corresponding ED profile, depicting the corrugation due to disordered amine-hydroxyl hydrogen-bonding.

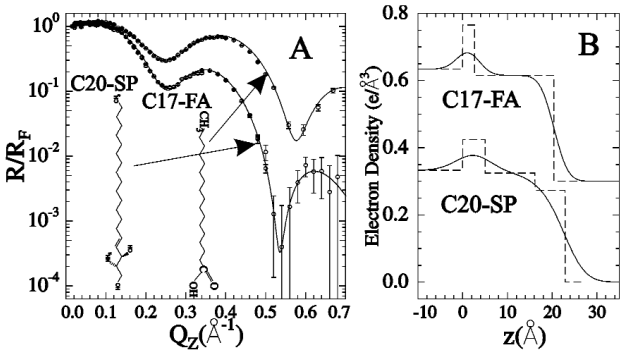

FIG. 3. A shows the normalized reflectivity R/R_F, (R_F is the calculated reflectivity for ideally flat water surface) of C20-sphingosine C17 fatty acid (margeric acid). The solid lines are calculated from the ED shown in B. In B, the dashed line is the ED with no interfacial smearing by surface roughness.

interface, as observed in x-ray reflectivity and GIXD experiments [5]. We have also shown that a metastable monolayer of C18-SP can be formed by spreading the material that is in excess at the interface to compensate for the dissolved molecules [7]. This process is similar to the one recently applied to short-chain alcohols, which are partially soluble in water [10]. On the other hand, according to its (π-*A*) isotherm, synthetic C20-sphingosine forms a more stable monolayer at aqueous interfaces. The ED for C20-sphingosine [see Fig. 2(B)] consists of three slabs. The one associated with the head group region is broader than the actual molecular head-group size, and the other two are associated with the acyl chains.

The intermediate slab has ED very close to that of crystalline alkanes, indicating that the chains in the middle slab are closely packed. Indeed, Bragg reflections, due to the ordering of the chains, are observed in the GIXD measurements, and their rod scans show that the length of the diffracting chains is consistent with the length of the intermediate slab extracted from the reflectivity. The top slab is lower in ED and does not contribute to the diffraction. It has been argued that the low density that is observed is due to corrugation or digitations of the chains into the gas interface. In our view, the chains conform to the strong and corrugated intermolecular binding at the head group region, which results from strong hydrogen bonds in the sphingosine head group [12, 13]. These bonds can occur at a few sites along the molecule, either regularly or randomly, leading to the digitations of the hydrocarbon tails. The three-slab model is, in fact, common to ceramide and sphingomyelin monolayers [6, 7]. To strengthen this point, Fig. 3(A) shows the normalized reflectivity of C20-sphingosine and of C17 fatty acid (margeric acid) at 20 mN/m at T = 19°C. The ED extracted from the reflectivity of margeric acid [shown in Figure 3(B)], like many other lipids, consists of only two homogeneous slabs, one associated with the head group region at the water interface, and the second due to the closely packed acyl chains, unlike the sphingolipids [5-7].

Micro-crystallization – Lipid-raft Precursor

The lateral organization of C18-SP and C20-SP in monolayers reinforces the conclusions from the reflectivity and the isotherms. The GIXD pattern (Qz = 0) of pure water surfaces is dominated by a broad peak at Q_{xy} = 1.94 Å^{-1}, due to the structure factor of the liquid surface, as shown in Fig. 4A. Spreading and compressing C18-SP or C20-SP monolayers slightly modifies the aqueous-surface structure factor, primarily in intensity. For C20-SP at finite pressures, a prominent sharp Bragg peak appears at Q_{xy} = 1.47 Å^{-1}. Figure 4B shows the same scan after the subtraction of the GIXD of pure water. Besides the Bragg peak, there is a negative broad minimum due to the modification of the water surface by the monolayer aforementioned. Applying a similar procedure to the C18-SP monolayer

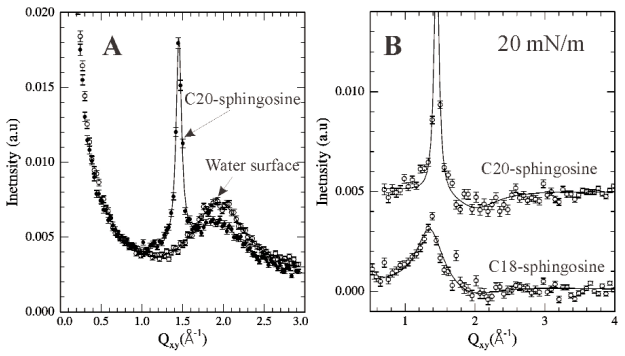

FIG. 4. A shows GIXD scans for a pure water surface (empty circles) and a C20-SP monolayer at the air-water interface (π = 20 mN/m). The fall-off in intensity at small angles is due to scattering from capillary waves at the interface, whereas the broad peak is due to the structure factor of the water surface, which we find to be slightly different than that of bulk water. B shows the GIXD from monolayers (after subtracting the contribution of water) for C20-SP and for C18-SP. Both monolayers show a very weak minimum around Q_{xy} = 2.0 Å^{-1}, indicating some reorganization of water at the interface due to head-group-water interaction.

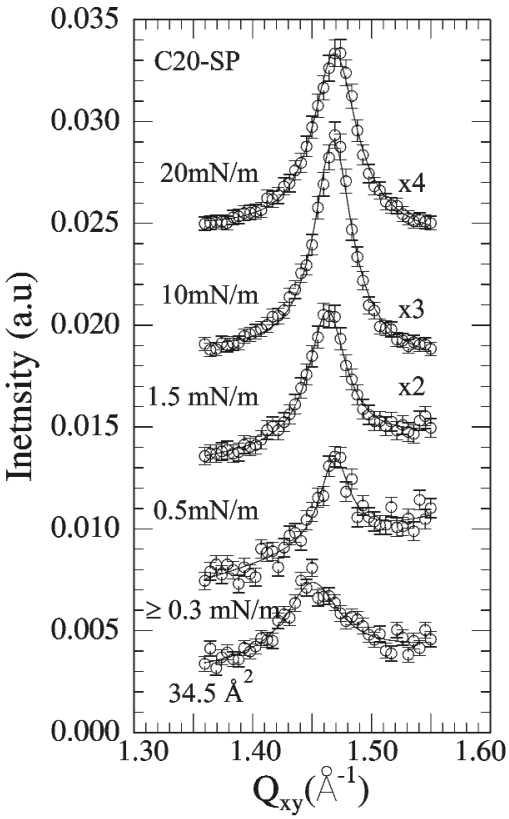

FIG. 5. Diffraction patterns (Q_z = 0) for C20-SP, showing the variation of the Bragg peak with surface pressure. Because of the spontaneous aggregation into nearly crystalline microdomains, a Bragg reflection is observed when the monolayer is spread at very low surface pressures.

yields, in addition to the modification of the water-surface structure factor, a broad peak centered at Q_{xy} = 1.38 Å^{-1}. The observation of a broad GIXD peak on and off the horizon for C18-SP, together with the rod scans, as shown in Fig. 4, indicates a short-range order with an average d-spacing of 4.8 Å. The out-of-plane GIXD peaks at different Q_z's (and their dependence on pressure) reveal a 2-D liquidlike state.

Figure 5 shows the variation of the in-plane diffraction pattern for various surface pressures. An important result in this respect is the Bragg reflection at very small surface pressures (below 0.3 mN/m) at an isothermal molecular area of ~34.5 Å^2, compared with 22.2-22.7 Å^2 extracted from the GIXD. This is strong evidence for the spontaneous aggregation of these molecules into crystalline microdomains at very low densities. Similar observations have been reported for C18-ceramide at the air-water interface [6, 7]. Such sphingolipid microdomains in cellular membranes can be the precursors of lipid-rafts to which proteins can be attached and that can be moved around to specific sites during signal transduction [4].

Surface x-ray studies of sphingosine monolayers revealed that condensation into nano 2-D crystals occurs at low densities and that the interface is corrugated as a result of the staggering of bound neighboring molecules [5-7]. These unique structural characteristics of sphingolipids were attributed to strong hydrogen bonds present in the head group region [13, 14]. It is argued that the marginal capability of C18-sphingosine to form a stable monolayer is very important for a molecule that mediates messages in the cell. In addition, the spontaneous microdomain formations and the corrugated interfaces of sphingolipid monolayers are consistent with the roles that sphingolipids play in the life cycle of eukaryotic cells and as the building blocks of specialized membranes. Sphingolipids, with their strong hydrogen bonds among nearest neighbors and with water molecules, tend to phase-separate from unsaturated lipids, giving to them the lateral mobility and solubility that can get them inside the cell in addition to the hydrophobic membrane. While it is tempting to associate the aggregation of sphingolipids [5-7] to lipid-rafts, it should be emphasized that it was suggested that the constituents of these rafts are glycosphingolipids and cholesterol [4], which are much more complicated systems than the simple sphingosines presented here.

Acknowledgments

I wish to thank D.S. Robinson for help at the APS. Ames Laboratory is operated for the U.S. Department of Energy (DOE) by Iowa State University under Contract No. W-7405-ENG-82. The MU-CAT sector at the APS is supported by the DOE Office of Science, Office of Basic Energy Sciences (BES), through Ames Laboratory under Contract No. W-7405-ENG-82. Use of the APS was supported by DOE BES under Contract No. W-31-109-ENG-38.

References

[1] S. Spiegel and A.H. Merrill, FASEB J. **10**,1388-1397 (1996).
[2] J.M. Hauser, B.M. Buehrer, and R.M. Bell, J. Biol. Chem. **269**, 6803-6809 (1994).
[3] Y.A. Hannun, J. Biol. Chem. **269**, 3125-3128 (1994).
[4] K. Simons and E. Ikonen, Nature **387**, 569-572, 1997.
[5] D. Vaknin, J. Am. Chem. Soc. **125**, 1313-1318 (2003).
[6] D. Vaknin and M.S. Kelley, Biophys. J. **79**, 2616-2623 (2000).
[7] D. Vaknin, M.S. Kelley, and B.M. Ocko, J. Chem. Phys. **115**, 7697-7704 (2001).
[8] D. Vaknin, in *Methods in Materials Research*, edited by N. Kaufmann, P. Abbaschian, P.A. Barnes, A.B. Bocarsly, C.-L. Chien, B.L. Doyle, B. Fultz, L. Leibowitz, T. Mason, and J. Sanchez (Wiley, New York, NY, 2001), p. 10d.2.1.
[9] J. Als-Nielsen and K. Kjaer, Proc. NATO Advanced Study Institute (ASI) Ser. B **211**, 113-138 (Plenum Publishing Corp., New York, NY, 1989).
[10] K. Kjaer, Physica B **184**, 100-109 (1994).
[11] B. Berge, J. Konovalov, J. Lajzerowicz, A. Renault, J.P. Rieu, M. Vallade, J. Als-Nielsen, G. Grübel, and J.F. Legrand, Phys. Rev. Lett. **73**, 1652-1655 (1994).
[12] H. Löfgren and I. Pascher, Chem. Phys. Lipids **20**, 273-284 (1977).
[13] K.S. Bruzik, Biochim. Biophys. Acta **939**, 315-326 (1988).